

# RELATIVE MANEUVERING FOR MULTIPLE SPACECRAFT VIA DIFFERENTIAL DRAG USING LQR AND CONSTRAINED LEAST SQUARES

Camilo Riano-Rios,<sup>\*</sup> Riccardo Bevilacqua,<sup>†</sup> and Warren E. Dixon<sup>‡</sup>

In this paper, a set of spacecraft consisting of multiple chasers and a single target is considered for rendezvous and along-orbit formation maneuvers. Each spacecraft can change its experienced drag acceleration by extending/retracting drag surfaces. First, the relative states of the linearized relative dynamics of each chaser-target pair are driven to zero using a Linear Quadratic Regulator (LQR). Then, a Constrained Least Squares (CLS) Problem is formulated to find the best achievable set of individual inputs to control all chasers under mutual constraints and actuator saturations. Tests using a multiple spacecraft simulation framework that includes  $J_2$  perturbation and the NRLMSISE-00 atmospheric density model, are conducted to validate the robustness of the proposed algorithm along with a method that uses the along-orbit formation as an intermediate stage to reduce the risk of potential collisions.

## INTRODUCTION

As interest in exploiting natural forces for orbital maneuvering increases due its potential for propellant cost savings, so is the use of fleets with several spacecraft for missions in Low Earth Orbit (LEO). The introduction of differential atmospheric drag for formation keeping control dates back to 1989. Using the Clohessy-Wiltshire (CW) linear model for the relative motion between two spacecraft, an algorithm was designed to control the in-plane motion by transforming the dynamics to a double integrator and a harmonic oscillator and taking advantage of closed form solutions that are valid when the relative drag is constant and, as consequence, the available inputs are assumed to be either a minimum, maximum or zero.<sup>1,2</sup>

Aerodynamic drag and lift were exploited to control in-plane and out-of-plane motion between two spacecraft.<sup>3</sup> In this work, a transformation of the CW linear model and closed form solutions were used to develop two control algorithms, one for the in-plane motion using only drag and the other for the out-of-plane motion using only lift. Based on the required drag and lift, an algorithm computed the orientation of a flat drag plate attached to each spacecraft. The Schweighart and Sedwick (SS)<sup>4</sup> linearized model for relative motion that includes the influence of the  $J_2$  perturbation

---

<sup>\*</sup> Ph.D Student, [crianorios@ufl.edu](mailto:crianorios@ufl.edu), Mechanical and Aerospace Department, University of Florida.

<sup>†</sup> Associate Professor, [bevilr@ufl.edu](mailto:bevilr@ufl.edu), Mechanical and Aerospace Department, University of Florida.

<sup>‡</sup> Ebaugh Professor, [wdixon@ufl.edu](mailto:wdixon@ufl.edu), Mechanical and Aerospace Department, University of Florida.  
939 Sweetwater Dr. MAE-A211, Gainesville FL, 32611-6250

has also been used to develop a control logic for rendezvous maneuvers between two spacecraft. The algorithm was based on closed form solutions and discrete inputs.<sup>5</sup>

A Lyapunov-based control strategy was implemented to achieve spacecraft rendezvous using differential drag.<sup>6</sup> The in-plane unstable SS dynamic model was initially stabilized using an LQR and then a Lyapunov-based controller was designed using the new stable dynamics, restricting the control command to discrete values. An adaptive capability to change controller parameters depending on the critical value of atmospheric drag was also implemented. In Reference 7, the spacecraft's attitude was used to change the experienced drag instead of using dedicated actuators for drag surfaces<sup>7</sup>. An LQR controller was designed to drive the system to a desired relative free motion using a state space representation of the error. The control command was then used to compute two angles that define a vector normal to the drag surface attached to the body and produce commands for an attitude determination and control system which was assumed available.

Research has also been conducted to include multiple spacecraft relative maneuvering. A centralized heuristic control logic was used to give priority to a specific chaser on a spacecraft fleet, then the target set its control command to meet the prioritized chaser's control requirements, (Reference 5). Only chasers that require the same sign for their inputs can meet their control command simultaneously. Others should remain with zero input until a new priority is established. In Reference 8, the formulation of an optimization problem was presented to find the minimum time required to achieve rendezvous with any number of spacecraft by using an augmented state space representation. Simulations with 2, 5 and 12 spacecraft were conducted using linearized dynamics.<sup>8</sup>

An adaptive sliding mode method was used to control the relative dynamics using differential drag.<sup>9</sup> The methodology was simulated for formation keeping as well as reconfiguration cases using two spacecraft. A heuristic algorithm for multiple spacecraft was developed and applied to an along-orbit formation keeping case with 4 spacecraft. In this algorithm, each chaser changes its drag acceleration to meet its control command, then the target changes its drag acceleration each orbit to sequentially meet the differential drag requirement of each chaser.

In this paper, we consider a fleet of several chasers maneuvering with respect to a single target to perform rendezvous and along-orbit formation maneuvers. Limitations in the control input, the coupling of the target's experienced drag with each chaser's relative drag acceleration computation, and possible priorities among chasers make this a constrained problem. We present a control framework that takes advantage of the spacecraft's capability to precisely control its experienced drag acceleration. First, an LQR is designed using the SS relative dynamics to drive all states to zero. Then, a Constrained Least Squares problem is formulated to compute the best set of achievable inputs for the fleet keeping all chasers under control as much as possible during the entire maneuver. Due to the presence of multiple chasers maneuvering in a relatively small area, a collision reduction algorithm is also presented.

The upcoming sections of the paper are organized as follows: First we describe the spacecraft relative dynamics, followed by a section describing the multiple spacecraft rendezvous algorithm, and then the problem is extended to the multiple spacecraft along-orbit formation algorithm. Sections that report simulation results and the collision risk reduction algorithm are also presented. Finally, a conclusion section presents the major outcomes of this work.

## **MODEL OF SPACECRAFT RELATIVE MOTION DYNAMICS**

Consider a fleet of multiple spacecraft where one is arbitrarily chosen as the target, and all other spacecraft are required to maneuver with respect to it. All spacecraft are assumed to have the capa-

bility to change their experienced drag acceleration by expanding/retracting controllable drag surfaces. They are also assumed to be on circular orbits and their relative distances are small if compared with the target's orbit radius.

### Equations for Relative Spacecraft Dynamics

A linearized model of a generic spacecraft moving with respect to a target on a circular orbit, including the  $J_2$  perturbation, was introduced by Schweighart and Sedwick (SS), and shown in equation (1).\*

$$\begin{aligned}\Delta\ddot{x} &= 2(\omega c)\Delta\dot{y} + (5c^2 - 2)\omega^2\Delta x + u_x \\ \Delta\ddot{y} &= -2(\omega c)\Delta\dot{x} + u_y \\ \Delta\ddot{z} &= -q^2\Delta z + 2lq\cos(qt + \phi) + u_z\end{aligned}\tag{1}$$

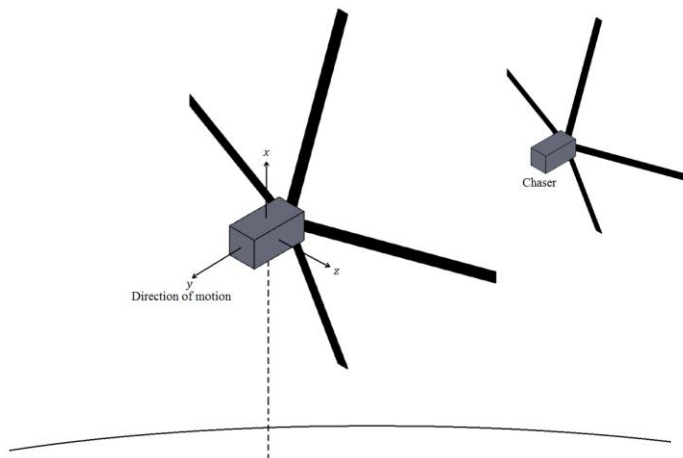


**Figure 1. Local-Vertical/Local-Horizontal coordinate system**

In Equation (1), the inputs  $[u_x \ u_y \ u_z]$  represent the components of the relative acceleration between the two spacecraft when a control action is applied, and the angular velocity of the target's circular orbit with respect to the inertial reference frame  $\omega$  is constant as well as the value of  $c$  given below.

$$c = \sqrt{1 + \frac{3\omega J_2 R_e^2}{8r_{ref}^2} (1 + 3\cos 2i_{ref})}\tag{2}$$

Also in Equation (1), the Local-Vertical/Local-Horizontal (LVLH) reference frame is used, and its attached coordinate system is shown in Figure 1. In Figure 1, the  $x$  axis points from the center of the earth towards the origin of the system (target's center of mass), the  $z$  axis is aligned with the orbit angular momentum vector and the  $y$  axis completes a right-hand Cartesian coordinate system.

---

\* See table of notation.

## Differential Drag

To control the experienced drag acceleration, each spacecraft has four drag surfaces each offset by 90 degrees with a fixed inclination of 20 degrees with respect to the rear face of the spacecraft. Since each surface can be expanded/retracted to change the cross-sectional area exposed to the incoming air flow, intermediate values are possible.

The drag surfaces' configuration is a simplified model of the Drag De-orbit Device (D3) designed at University of Florida ADvanced Autonomous MULTiple Spacecraft (ADAMUS) Lab.<sup>10,11,12,13</sup> The acceleration due to atmospheric drag experienced by a spacecraft's surface ( $a_{d,j}$ ) can be expressed as follows.

$$a_{d,j} = -\left(\frac{\rho S C_D}{2m} V_{\perp,j}^2\right) \hat{n}_{\perp,j} \quad (3)$$

For our purposes, the drag surfaces will always be homogeneously deployed to achieve a desired drag acceleration, then the only non-zero component of  $a_{d,j}$  is opposite to the direction of the spacecraft's velocity vector ( $\hat{V}$ ), as shown in equation (4). Note that the drag acceleration experienced by the target ( $u_t$ ) and the  $i^{th}$  chaser ( $u_{c,i}$ ) are along the  $y$  direction of the LVLH coordinate system. Thus, the relative drag of a chaser with respect to the target is also along this direction and is given by equation (5), making  $u_y = \Delta u_i$  the only non-zero input to the SS equations (1). The dynamics along the  $z$  direction and in-plane are decoupled, which makes only the in-plane ( $x$ - $y$ ) motion controllable by means of atmospheric drag.

$$u = \sum_{j=1}^4 -\left(\frac{\rho S C_D}{2m} V_{\perp,j}^2 \cos(20^\circ)\right) \hat{V} \quad (4)$$

$$\Delta u_i = u_t - u_{c,i} \quad (5)$$

A summary of the modeling assumptions considered for the purpose of this study are listed below.

1. All spacecraft in the fleet are attitude stabilized by other means.
2. All spacecraft in the fleet have the same drag coefficient  $C_D$  and mass  $m$ .
3. Only the in-plane motion is considered for relative maneuvering, then the state vector for a Chaser/Target pair is  $[\Delta x \ \Delta \dot{x} \ \Delta y \ \Delta \dot{y}]^T$ .
4. Target is in circular orbit
5. The relative distances are small compared to the target's orbit radius. This allows to use the linear time invariant set of SS equations (1). To guarantee this assumption, we make use of orbital elements to establish bounds for the possible initial conditions of any chaser:

$i^{th}$  Chaser's Semi-major axis = Target's Semi-major axis +/- 0.5 km

$i^{th}$  Chaser's Eccentricity = Target's Eccentricity +  $5 \times 10^{-5}$

$i^{th}$  Chaser's Inclination = Target's Inclination

$i^{th}$  Chaser's RAAN = Target's RAAN

$i^{th}$  Chaser's Argument of perigee = Target's Argument of perigee

$i^{th}$  True anomaly = Target's True anomaly +/- 0.03 degrees.

## MULTIPLE SPACECRAFT RENDEZVOUS CONTROL ALGORITHM

In this section, we consider a fleet with  $N$  chasers and a single target to perform rendezvous using an LQR. The Constrained Least Squares (CLS) approach is then presented to include constraints associated with actuation limitations, the presence of multiple chasers maneuvering simultaneously, and priority among chasers.

### Single Chaser/Target Case

For the two-spacecraft case we consider the in-plane relative dynamics between the  $i^{th}$  chaser and the target derived from Equation (1) as follows.

$$\dot{X}_i = A_i X_i + B_i \Delta u_i \rightarrow \begin{bmatrix} \Delta \dot{x}_i \\ \Delta \ddot{x}_i \\ \Delta \dot{y}_i \\ \Delta \ddot{y}_i \end{bmatrix} = \begin{bmatrix} 0 & 1 & 0 & 0 \\ b & 0 & 0 & a \\ 0 & 0 & 0 & 1 \\ 0 & -a & 0 & 0 \end{bmatrix} \begin{bmatrix} \Delta x_i \\ \Delta \dot{x}_i \\ \Delta y_i \\ \Delta \dot{y}_i \end{bmatrix} + \begin{bmatrix} 0 \\ 0 \\ 0 \\ 1 \end{bmatrix} \Delta u_i \quad (6)$$

$$a = 2(\omega c) \quad b = (5c^2 - 2)\omega^2$$

The eigenvalues of the system are:  $[0 \ 0 \ \sqrt{b - a^2} \ (-\sqrt{b - a^2})]^T$  where  $(b - a^2)$  is a negative constant. Therefore, all eigenvalues of the system are on the imaginary axis. By inspecting the Jordan normal form of the state transition matrix  $A_i$  it turns out that the system is unstable. The controllability of the system can also be determined by evaluating the controllability matrix, which is full rank, then the system is controllable.

Let us first consider the rendezvous problem where the desired final state vector is  $[0 \ 0 \ 0 \ 0]^T$ . Therefore, a regulator is sufficient to meet this condition. The LQR is an interesting approach for this problem because it provides an optimal feedback control law that considers the desired performance for each state and the available control input. It is also considered a robust regulator.<sup>14</sup> The feedback control law provided by the LQR has the form in Equation (7), and is obtained by minimizing the cost function shown in Equation (8).

$$\Delta u_i = -K_{LQR} X_i \quad (7)$$

$$J = \int_0^\infty (X_i^T Q X_i + \Delta u_i^T R \Delta u_i) dt \quad (8)$$

where  $Q = Q^T \geq 0 \in \mathbb{R}^{4 \times 4}$  and  $R > 0$  is a scalar. The weights  $Q$  and  $R$  are used to establish the desired performance for each state and available control effort respectively, then a trade-off between them exists in  $J$ . To determine values for  $Q$  and  $R$  several simulations were conducted with different initial conditions using spacecraft characteristics similar to those in Reference 5 and constant atmospheric density (Table 1), as result we set  $R = 1.8 \times 10^{16}$  and  $Q = \text{diagonal}(180, 1, 1.8, 1)$ . The high value of  $R$  penalizes the control effort term. This is desirable considering the amplitude limitations of relative drag acceleration. Values on the main diagonal of  $Q$  were selected to prioritize the reduction of position error along the  $x$  direction, which in our simulations was the state that required more control effort to be stabilized.

The matrix  $K_{LQR}$  can be obtained by solving the Algebraic Riccati Equation (ARE) for  $P$  and using the constant gain matrix definition, Equation (9).

$$A^T P + PA - PBR^{-1}B^T P + Q = 0 \quad (9)$$

$$K_{LQR} = R^{-1}B^T P$$

**Table 1. Spacecraft characteristics and atmospheric density**

|  |                        |
|--|------------------------|
| Mass, [kg]                             | 10                     |
| $S$ , [ $m^2$ ]                        | 1                      |
| $C_D$                                  | 2.2                    |
| Altitude $h$ , [km]                    | 350                    |
| $\rho_{350 \text{ km}}$ , [ $kg/m^3$ ] | $6.98 \times 10^{-12}$ |
| $i_{ref} = i_{ss}$ , [deg]             | 51.595                 |

The LQR was capable of reducing the relative state errors even when the input is saturated, remaining stable and keeping the system under conditions where the SS linearized equations are still valid. The saturation function used is shown in equation (10). Note that  $\Delta u_{i,min}$  and  $\Delta u_{i,max}$  values vary in time depending on the atmospheric density experienced by the  $i^{th}$  chaser and the target. Results from tests to validate stability under saturation are presented in the simulations section.

$$\Delta u_i = \begin{cases} \Delta u_{i,max} & , \quad \Delta u_i > \Delta u_{i,max} \\ \Delta u_{y,i} & , \quad \Delta u_{i,min} < \Delta u_i < \Delta u_{i,max} \\ \Delta u_{i,min} & , \quad \Delta u_i < \Delta u_{i,min} \end{cases} \quad (10)$$

### Multiple Chasers and One Target Case

When multiple chasers are maneuvering with respect to a single target, it is necessary to consider the resulting impact on the achievable levels of relative drag. Since the drag acceleration experienced by the target spacecraft is involved in the calculation of relative drag for every chaser/target subsystem, the system becomes constrained. A case could exist where the target cannot meet the relative drag required by all chasers at a specific time instant. In this situation, the development of an algorithm to determine the set of inputs to apply becomes necessary.

Our goal is the development of a strategy capable of managing any number of chasers without human intervention while considering mutual constraints and actuation limitations. To address this problem, heuristic algorithms are usually implemented to make the target switch among chasers and meet their control input requirements during specific periods of the entire maneuver. The switching laws heavily depend on the application and some examples can be found in References 5 and 9. The main problem with these switching algorithms is that some chasers can drift away from the target while it is giving priority to others in the fleet, this is undesirable especially when there are several chasers.

One of the main advantages of the D3 device is that each drag surface can achieve intermediate positions. This feature allows us to achieve a required relative drag through several deployment combinations between the involved spacecraft which makes the multiple spacecraft problem less restrictive than cases where only discrete inputs are considered. The first idea that may arise is to deploy the drag surfaces on the target spacecraft halfway so that all chasers can achieve positive and negative relative drag values. This approach may be too restrictive because the input saturation

limits become smaller for all spacecraft during the entire maneuver. Given the constraints already existing in the system, a less restrictive algorithm to find a good set of individual inputs is desirable.

For the multiple spacecraft problem each single chaser/target pair corresponds to a set of SS equations (1) that must be driven to the desired state by using the LQR control law. The relative drag acceleration is the input to the system that is computed using the LQR. Let  $U_d = [\Delta u_1, \Delta u_2, \Delta u_3 \dots \Delta u_N]^T$  be a vector that contains the desired control inputs in a fleet of  $N$  chasers and one target, and  $U_{ind} = [u_t, u_{c,1}, u_{c,2}, \dots, u_{c,N}]^T$  the vector that contains the individual input (drag acceleration) of all spacecraft, including the target ( $u_t$ ). We can also express a linear system that represents the relationship between these vectors (Equation (11)).

$$CU_{ind} = U_d,$$

$$\begin{bmatrix} 1 & -1 & 0 & 0 & 0 & 0 \\ 1 & 0 & -1 & 0 & 0 & 0 \\ 1 & 0 & 0 & -1 & 0 & 0 \\ 1 & 0 & 0 & 0 & \ddots & 0 \\ 1 & 0 & 0 & 0 & 0 & -1 \end{bmatrix} \begin{bmatrix} u_t \\ u_{c,1} \\ u_{c,2} \\ u_{c,3} \\ \vdots \\ u_{c,N} \end{bmatrix} = \begin{bmatrix} \Delta u_1 \\ \Delta u_2 \\ \Delta u_3 \\ \vdots \\ \Delta u_N \end{bmatrix} \quad (11)$$

The ideal case would be that the left-hand-side is equal to  $U_d$ , but sometimes this is not because of the constraints associated with the multiple spacecraft problem and input saturations. Therefore, a reasonable approach is to minimize the error between both sides of Equation (11) when subject to constraints. A technique that allows us to formulate the problem in that way is the CLS approach, which in our case is formulated as follows.

$$\min_{U_{ind}} \frac{1}{2} \|CU_{ind} - U_d\|_2^2 \quad \text{such that} \quad \begin{cases} 1. & u_t - u_{c,p} = U_d(p) \\ 2. & u_{min,t} \geq u_t \geq 0 \\ 3. & u_{min,i} \geq u_{c,i} \geq 0 \quad i = 1, \dots, N \end{cases} \quad (12)$$

In Equation (12),  $U_d(p)$  is the desired relative drag between the  $p^{th}$  chaser and the target, represented as the  $p^{th}$  position of vector  $U_d$ . The constraints in Equation (12) represent the following attributes.

1. Priority to the  $p^{th}$  chaser which allows this chaser to behave as in the single chaser/target case,
2. Saturation for the target,
3. Saturation for chasers.

The saturation bounds can be time varying to account for changes in the atmospheric density. For a real operation case, estimates for these bounds can be obtained by performing a simulation prior to the actual maneuver using the NRLMSISE-00 density model with predictions of F10.7 and  $A_p$  indices, which are available online.

The CLS approach provides the  $U_{ind}$  that makes the error as small as possible when using the Least Squares algorithm. For simulation purposes, the CLS is evaluated each time step using the *lsqlin* command in MATLAB which has shown to be computationally light. It has an average computation time for a six spacecraft case of 0.0039 seconds using an Intel Xeon W3530 CPU at  $2.8GHz \times 4$ . Note also that it is independent of the control technique used to determine the desired

values of relative drag ( $U_d$ ). This feature makes the simulation suitable for controller performance comparison purposes.

## MULTIPLE SPACECRAFT ALONG-ORBIT FORMATION ALGORITHM

In this section we consider an along-orbit formation where the chasers are required to be along the target's orbit with specific separations ( $\Delta d$ ). To achieve this type of formation we use the same LQR + CLS approach with slight changes in the relative states used for the SS equations.

### Change of Reference Frame

For the rendezvous problem the LVLH reference frame was used to compute the relative states of each chaser with respect to the target. This reference frame allowed us to use the LQR to regulate the chasers to the target's position. Let us consider for the along-orbit formation a reference frame that has an offset with respect to the LVLH but still moves with the target.

A desired distance with respect to the target ( $\Delta d_i$ ) along its orbit is given to the  $i^{th}$  chaser in the fleet. This distance needs to be consistent with the assumption of small inter-spacecraft distances for the SS equations to remain valid. Note that for the along-orbit formation case the distance  $\Delta d_i$  can be expressed as an offset in true anomaly ( $\Delta\theta_i$ ) from the target's orbital elements representation as shown in Equation (13).

$$\Delta\theta_i = \frac{\Delta d_i}{a_t} [rad] \quad (13)$$

In Equation (13),  $a_t$  is the target's semi-major axis, then the orbital elements for the origin of the new reference frame are simply the same as for the target but adding the offset  $\Delta\theta_i$  to the true anomaly. The  $i^{th}$  coordinate system is defined by the  $x_i$  axis pointing from the center of the earth towards the origin of the system (desired position for  $i^{th}$  chaser), the  $y_i$  axis pointing along the orbital track with the  $z_i$  axis completing a right-hand Cartesian coordinate system as shown in Figure 2.

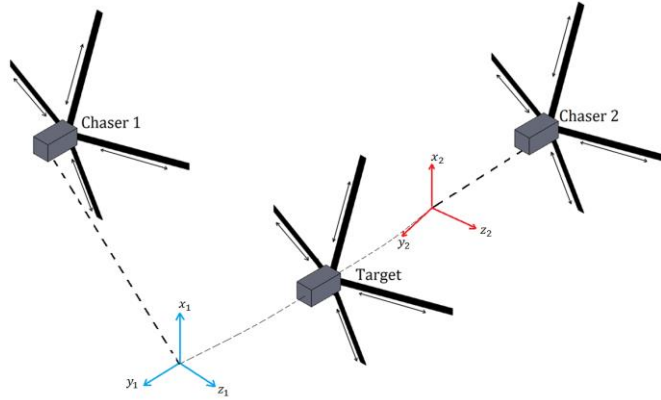


**Figure 2. New coordinate systems**

Each set of SS equations represent relative states with respect to the desired position and the goal remains the same as in the rendezvous case. Therefore, the LQR+CLS approach remains valid for along-orbit formation.



## SIMULATION RESULTS

This section presents the simulation framework used for testing the LQR+CLS algorithm and results for two sample cases: rendezvous maneuver of a fleet with six spacecraft (five chasers and one target), and along-orbit formation maneuver of a fleet with seven spacecraft (six chasers and one target).

To validate the approaches presented in previous sections, a MATLAB-based simulation was developed to demonstrate the LQR and the CLS algorithms while integrating the nonlinear dynamics for each spacecraft. The nonlinear dynamic equations including the  $J_2$  perturbation, expressed in the Earth-Centered Inertial (ECI) reference frame are

$$\begin{aligned}\ddot{x} &= -\frac{\mu}{r^3}x + \frac{3}{2}\left(\frac{J_2\mu R_e^2}{r^4}\right)\left(\frac{x}{r}\left(\frac{5z^2}{r^2} - 1\right)\right) + U_x \\ \ddot{y} &= -\frac{\mu}{r^3}y + \frac{3}{2}\left(\frac{J_2\mu R_e^2}{r^4}\right)\left(\frac{y}{r}\left(\frac{5z^2}{r^2} - 1\right)\right) + U_y \\ \ddot{z} &= -\frac{\mu}{r^3}z + \frac{3}{2}\left(\frac{J_2\mu R_e^2}{r^4}\right)\left(\frac{z}{r}\left(\frac{5z^2}{r^2} - 3\right)\right) + U_z\end{aligned}\quad (14)$$

where  $[U_x, U_y, U_z]$ , are the components of the drag acceleration experienced by each spacecraft. Note that when expressed in the Earth-Centered Inertial (ECI) reference frame the drag acceleration has components on the three axes. The set of equations in (14) is integrated for each spacecraft using the variable step ODE45 algorithm.

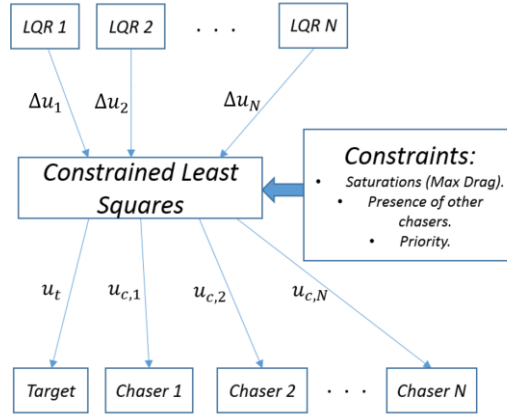


**Figure 3. LQR+CLS Implementation**

At each time step the relative states required for Equation (6) are obtained by making the transformation to LVLH (or reference frames at desired locations) of each chaser spacecraft.<sup>15</sup> The LQR control inputs are computed using Equation (7) and then used as desired relative drag acceleration in the CLS algorithm (Figure 3). Finally, the resulting individual accelerations are transformed to ECI and applied in Equation (14). The CLS algorithm in Equation (12) dynamically changes the limit values of saturations in constraints 2 and 3 due to the variable atmospheric density.

The NRLMSISE-00 atmospheric density model is implemented in the simulation through the built-in MATLAB command *atmosnrlmsise00*. This model takes into consideration spacecraft position (Latitude, Longitude, Altitude), date, time, solar flux index (F10.7) and geomagnetic index (Ap). F10.7 and Ap are available online.

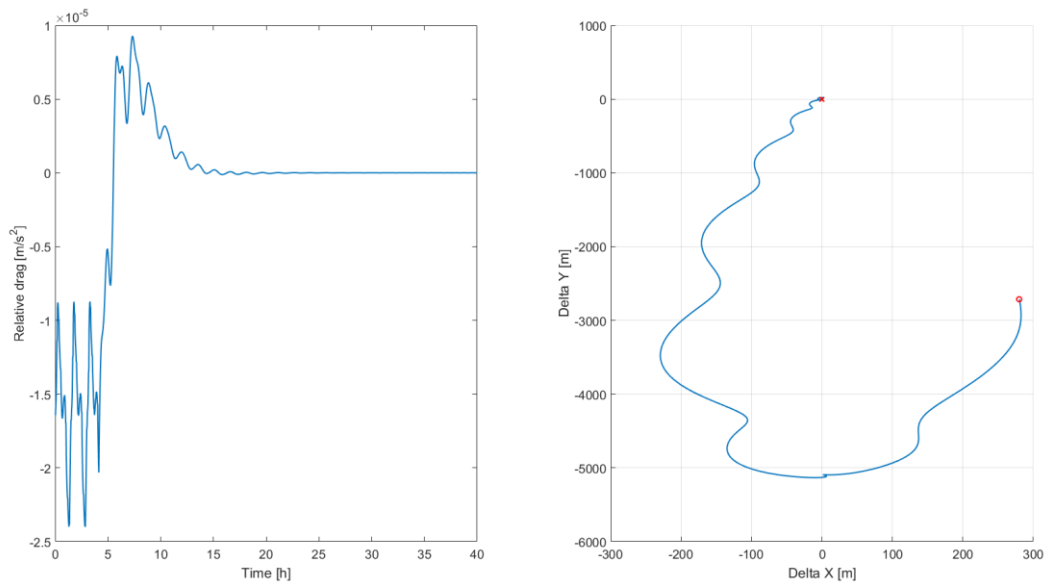


**Figure 4. LQR under saturation, simulation result example**

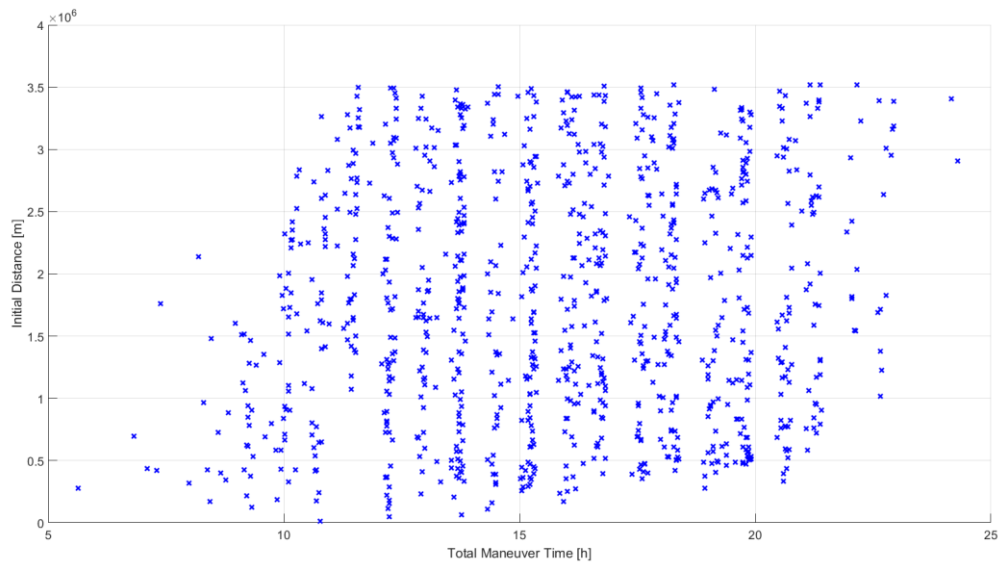


**Figure 5. LQR under saturation (1000 Simulations)**

## LQR Performance under Actuator Saturation

To evaluate performance of the designed LQR regulator, one thousand simulations were conducted including  $J_2$  perturbations and the NRLMSISE-00 atmospheric density model. Figure 4 shows an example of the saturated relative drag acceleration applied by the LQR to achieve rendezvous state. Note that saturation is time varying due to changes in atmospheric density. Results for all simulations are presented in Figure 5 showing that in all cases the regulator was able to complete the rendezvous maneuver.

## Multiple Spacecraft Rendezvous Maneuver Simulation

A fleet of six spacecraft is considered for a rendezvous maneuver. This number of spacecraft has been selected to show the system's performance under constraints imposed by multiple chasers and will also help to illustrate the collision reduction algorithm later. As mentioned in previous sections, all spacecraft are assumed to have the same physical properties and five of them are maneuvering with respect to one that is considered the target. The initial conditions (orbital elements) for the target are presented in Table 2, and are similar to those of the International Space Station (ISS). Because the simulation case is not considering priority for any of the chasers, the first constraint in Equation (12) is not used.

Initial conditions for the five chasers are randomly generated and shown in Table 3 following the restrictions on the orbital elements presented in the model of relative dynamics section to ensure small inter-spacecraft initial distances.

**Table 2. Orbital elements of the target**

|                |               |
|----------------|---------------|
| $a_{ISS}$      | 6713889.83 m  |
| $e_{ISS}$      | 0             |
| $i_{ISS}$      | 51.94116 deg  |
| $\Omega_{ISS}$ | 206.35768 deg |
| $\omega_{ISS}$ | 101.07112 deg |
| $\theta_{ISS}$ | 108.08480 deg |

**Table 3. Orbital elements of all chasers, rendezvous case**

| Parameter                | Chaser 1   | Chaser 2   | Chaser 3   | Chaser 4   | Chaser 5   |
|--------------------------|------------|------------|------------|------------|------------|
| $a$ [m]                  | 6714182.03 | 6714349.32 | 6714238.95 | 6714147.57 | 6714045.31 |
| $e$ ( $\times 10^{-5}$ ) | 2.1088     | 3.2787     | 4.6700     | 3.7157     | 0.85593    |
| $i$ [deg]                | 51.94116   | 51.94116   | 51.94116   | 51.94116   | 51.94116   |
| $\Omega$ [deg]           | 206.35768  | 206.35768  | 206.35768  | 206.35768  | 206.35768  |
| $\omega$ [deg]           | 101.07112  | 101.07112  | 101.07112  | 101.07112  | 101.07112  |
| $\theta$ [deg]           | 108.1114   | 108.0541   | 108.0942   | 108.0770   | 108.0999   |

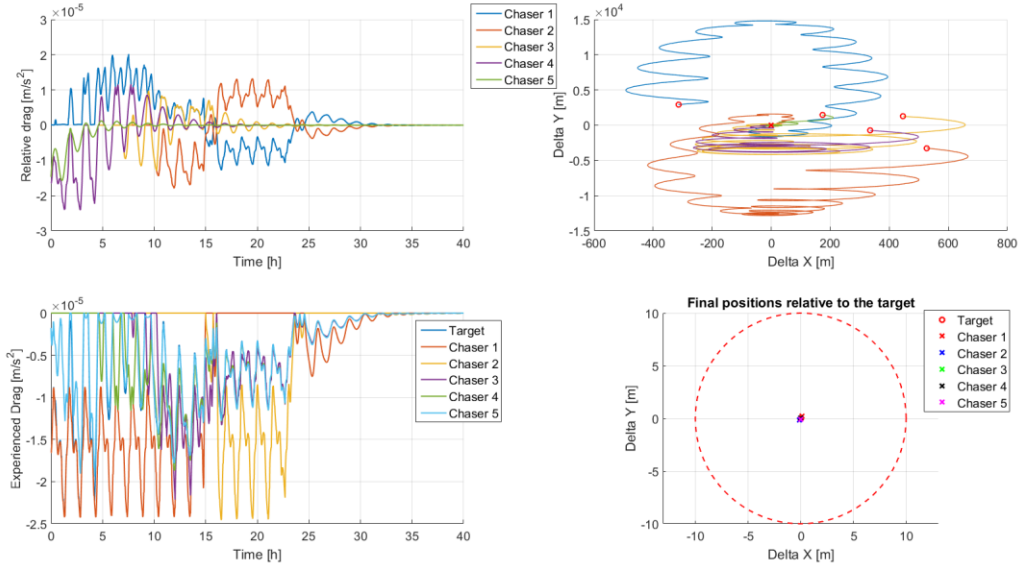


**Figure 6. Simulation results for the rendezvous case with six spacecraft**

Simulation results for the rendezvous case are shown in Figure 6. Note that all relative drag accelerations experience time varying saturation due to the changes in atmospheric density (top-left). The individually experienced drag accelerations (bottom-left) are also saturated and negative as expected from Equation (4). The action of the CLS approach can be observed in the drag acceleration acting on the target spacecraft, which is changing in time to help minimize the error between the desired relative inputs and the achievable ones. For simulation purposes we consider that a chaser achieves rendezvous when it enters and remains inside a 10 meter circle around the origin. Therefore, the LQR+CLS approach has shown its capability to stabilize all chasers in 30.3 hours under nonlinearities, perturbations, and mutual constraints.

### Multiple Spacecraft Along-Orbit Maneuver Simulation

To illustrate how the proposed approach addresses the along-orbit formation problem, we consider again a fleet of six spacecraft with one of them randomly selected as the target. The simulation framework has been programmed in such a way that the user can straightforwardly change the number of chasers and the desired inter-spacecraft separation. The simulator then automatically changes the dimension of all sub-routines and propagates the dynamics. For this simulation, the orbital elements in Table 2 are used for the target's initial conditions and those for the chasers are randomly generated (Table 4). The inter-spacecraft distance is set to 2 km with three chasers behind and the other three ahead of the target's position.

**Table 4. Orbital elements of all chasers, formation case**

| Parameter                | Chaser 1   | Chaser 2   | Chaser 3   | Chaser 4   | Chaser 5   |
|--------------------------|------------|------------|------------|------------|------------|
| $a$ [m]                  | 6713421.66 | 6713486.96 | 6713706.93 | 6713828.57 | 6714185.03 |
| $e$ ( $\times 10^{-5}$ ) | 1.3846     | 4.1173     | 3.6016     | 1.9078     | 0.9344     |
| $i$ [deg]                | 51.94116   | 51.94116   | 51.94116   | 51.94116   | 51.94116   |
| $\Omega$ [deg]           | 206.35768  | 206.35768  | 206.35768  | 206.35768  | 206.35768  |

|                |           |           |           |           |           |
|----------------|-----------|-----------|-----------|-----------|-----------|
| $\Omega$ [deg] | 101.07112 | 101.07112 | 101.07112 | 101.07112 | 101.07112 |
| $\theta$ [deg] | 108.0598  | 108.0942  | 108.0541  | 108.0999  | 108.0828  |

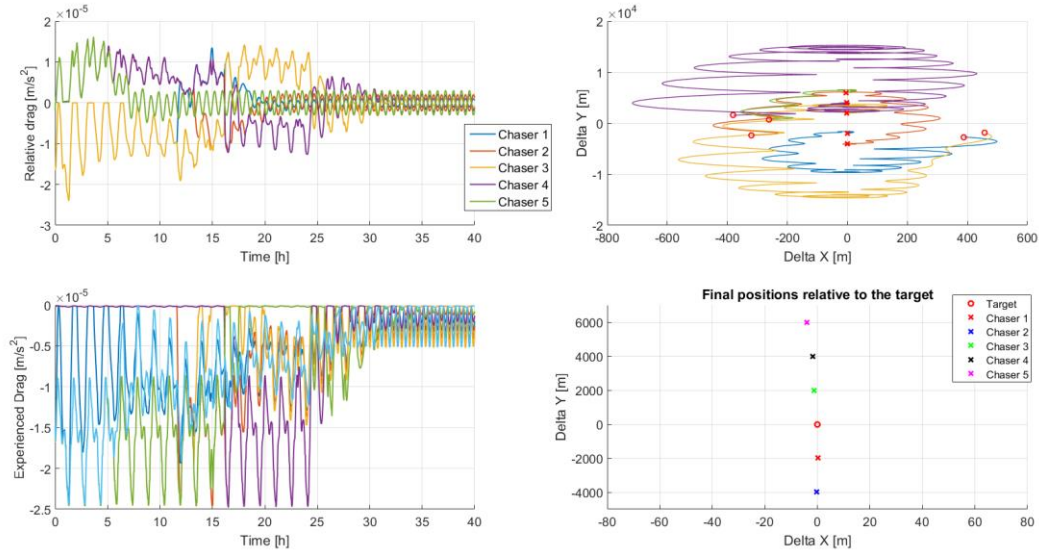


**Figure 7. Simulation results for the along-orbit formation case with six spacecraft**

Figure 7 shows the simulation results for the along-orbit formation example. As in the rendezvous case, relative and individual drag accelerations are saturated due to the variations in atmospheric density. Relative drag accelerations do not converge to zero because each chaser needs to keep making corrections to remain in the same relative position with respect to the target. If zero input is given once stabilized, chasers would start drifting apart from the target in accordance with the SS equations. Using the same criteria of a 10 meter circle around the desired final positions, the LQR+CLS approach is capable of stabilizing all chasers in a formation configuration in 34.9 hours.

## COLLISION RISK REDUCTION

The presence of multiple spacecraft maneuvering at relatively small distances increase the risk of possible collisions. In this section, some observations about collisions along with a preliminary approach to reduce the collision risk between spacecraft in the fleet are presented.

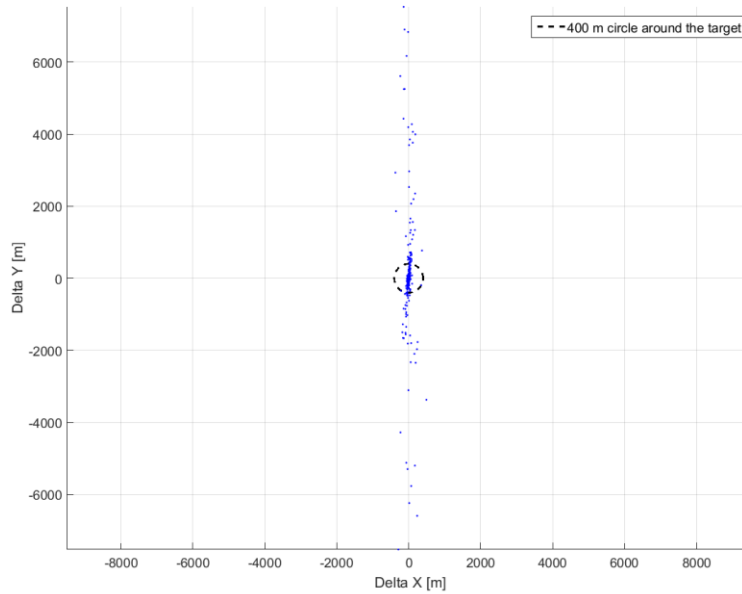


**Figure 8. Collision locations for one thousand simulation runs, five chasers**

As can be observed from Figure 6 and Figure 7, the LQR+CLS approach tends to make chasers follow similar paths. Moreover, due to the LQR features, all chasers tend to be in proximity to the target during a significant period of the total maneuver time. This makes collisions between chasers more likely to occur near to the target, especially in rendezvous maneuvers. To evaluate collisions, each spacecraft is assumed to be a circle of 10 meters diameter, this assumption was made to account for possible errors between the simulations and reality. One thousand simulations with random initial conditions for five chasers rendezvous maneuvers were performed to better observe this behavior. Figure 8 shows that from the total number of collisions, 97.1% were inside a circle of 400 meters radius around the target.

Due to the high uncertainty in the atmospheric density, the presence of nonlinearities, perturbations and the amplitude limitations of atmospheric drag, collision avoidance by means of relative drag becomes a difficult problem. Path prediction for each chaser with high degree of accuracy would be required to identify possible collisions with enough time of anticipation in order to avoid them. Considering this fact and our observations, we propose the use of along-orbit formation as the first stage of a multiple spacecraft rendezvous maneuver. This would introduce shape changes on chasers' paths reducing collision risk due to path similarities. A second stage to complete the rendezvous maneuver that consists in driving the modified reference frames to the target's position, is also presented along with simulation results to evaluate its performance.

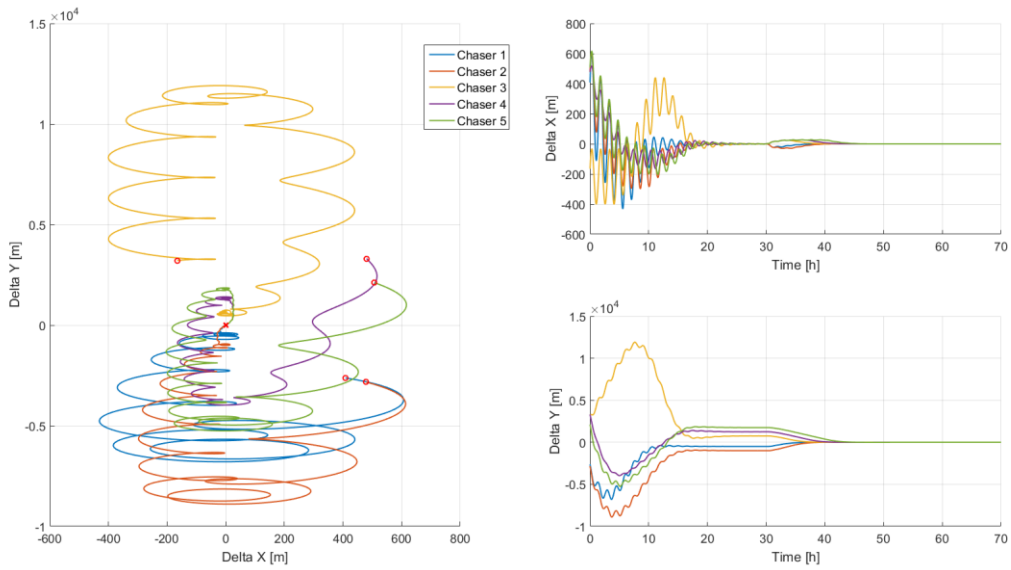


**Figure 9. Rendezvous maneuver with collision risk reduction, five chasers example**

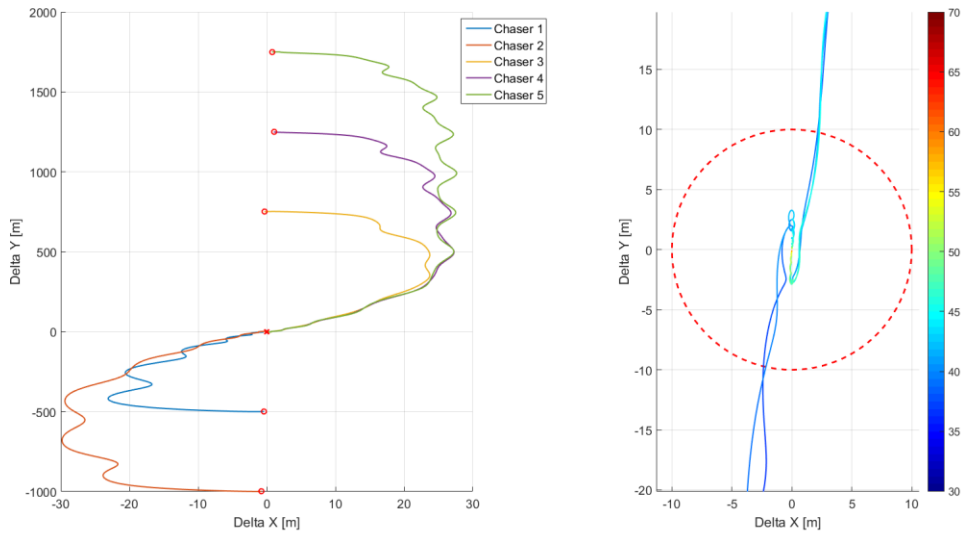


**Figure 10. Last stage of the rendezvous maneuver with collision risk reduction**

### Along-orbit Formation for collision reduction

Given the results shown in Figure 8, our approach is intended to reduce collisions near the target during rendezvous maneuvers, these collisions can be reduced by first stabilizing the chasers along the target's orbit and then driving all the modified reference frames to the actual LVLH position at the same rate. To illustrate this idea, Figure 9 shows results for a rendezvous maneuver with five

randomly initialized chasers and inter-spacecraft distance of 500 meters. The last stage of the maneuver (Figure 10) shows the path that each chaser follows when the reference frames are driven to the target's position. Although the paths are similar (left), each chaser arrives to the rendezvous state at a different time (right). The complete rendezvous maneuver time was 45.1 hours and collisions were reduced from five to zero.

Note that the desired along-orbit positions were selected in such a way that half of all chasers are ahead and the other half are behind the target. An extra offset of 250 meters was added to the desired positions ahead of the target to ensure that each chaser achieves the rendezvous at different time. One thousand simulations for rendezvous maneuvers with five chasers were performed to evaluate the collision reduction algorithm, each iteration simulates cases with and without collision reduction for the same set of initial conditions, resulting in the number of collisions reported in Table 5. Although the maneuvering time increases by including this algorithm, the total number of collisions was reduced by 95.21%.

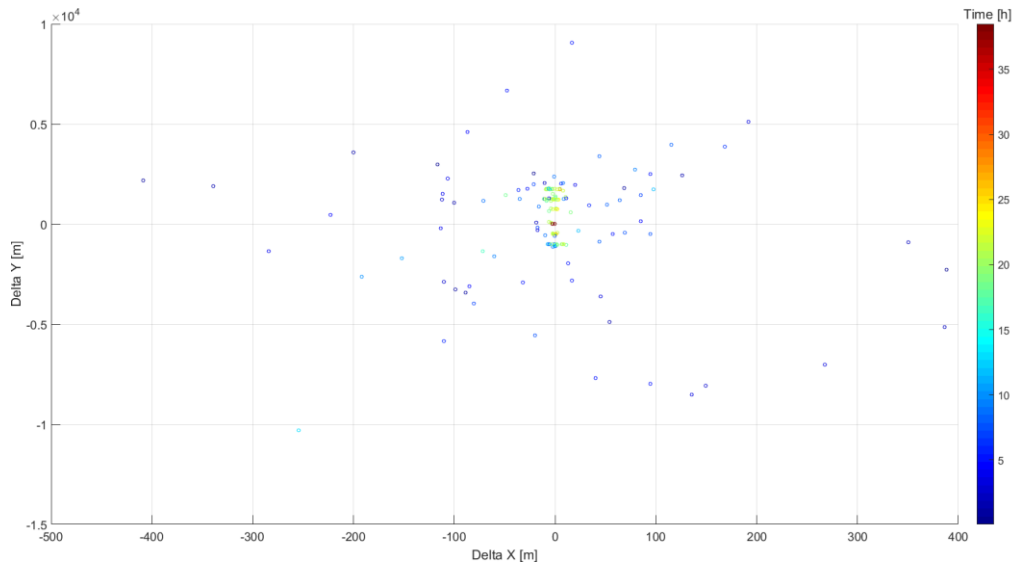


**Figure 11. Results after 1000 simulation runs with collision reduction algorithm, 5 Chasers**

Figure 11 shows the locations relative to the target's position where collisions occurred, and the corresponding time is represented by colors. An interesting result is that all the remaining collisions occur before the chasers are stabilized along the target's orbit. Therefore, once chasers are along the same orbit, the algorithm is able to drive all chasers to rendezvous without collision risk.

**Table 5. Total number of collisions after 1000 simulation runs**

|                                       |                 |
|---------------------------------------|-----------------|
| Without collision reduction algorithm | 3257 collisions |
| With collision reduction algorithm    | 156 collisions  |
| Reduction                             | 95.21%          |

## CONCLUSION

A novel strategy for multiple spacecraft relative maneuvering using differential drag has been tested for rendezvous and along-orbit missions with up to five chasers. Results of numerical simulations using nonlinear dynamics with perturbations and the NRLMSISE-00 atmospheric density



model have shown the LQR+CLS algorithm's robustness with respect to unmodeled dynamics and constraints among spacecraft in the fleet. The simulation illustrates the capability to simultaneously manage any number of chasers considering input saturations and priority for a specific chaser if required.

The definition of modified reference frames was presented as a first approach to reduce the risk of potential collisions during the maneuver, especially when a rendezvous mission is required. Results from one thousand simulation tests of rendezvous maneuvers with five chasers have shown an important reduction in the total number of collisions. Nevertheless, the presence of collisions is still a concern. To address this problem we are currently working on an algorithm to determine the slot for each chaser along the target's orbit in such a way that the collision risk is also reduced at that stage.

The ADAMUS' D3 design capable of individually deploying very long drag surfaces can also be used to change aerodynamic and gravity gradient torques for attitude control. The simulation framework presented in this paper provides the opportunity to integrate future attitude control algorithms, and test their performance under the multiple spacecraft constraints.

## NOTATION

|            |   |
|------------|---|
| $A_p$      | Geomagnetic index   |
| $a$        | Constant coefficient in the state transition matrix   |
| $a_{d,j}$  | Magnitude of drag acceleration for the $j^{th}$ spacecraft's drag surface   |
| $A_i, B_i$ | State space representation matrices for the $i^{th}$ chaser-target pair   |
| $b$        | Constant coefficient in the state transition matrix   |
| $C$        | Matrix used to relate $U_{ind}$ and $U_d$ in the CLS approach   |
| $c$        | Coefficient in Schweighart-Sedwick equations  |
| $C_D$      | Drag coefficient  |
| F10.7      | Solar flux index  |
| $i_{ref}$  | Reference local-vertical/local-horizontal orbit inclination   |
| $J$        | Cost function in the LQR formulation  |
| $J_2$      | Second-order harmonic of Earth's gravitational potential field (Earth Flattening)<br>( $108,263 \times 10^{-8}$ ) |
| $K_{LQR}$  | Constant gain matrix obtained from LQR formulation  |
| $l$        | Coefficient in the Schweighart-Sedwick equations (out-of-plane motion)  |
| $m$        | Spacecraft's mass   |
| $\mu$      | Earth's gravitational parameter   |

|                                      |  |
|--------------------------------------|--|
| $N$                                  | Number of chasers in the fleet   |
| $\hat{n}_{\perp,j}$                  | Unit vector normal to the $j^{th}$ drag surface  |
| $P$                                  | Matrix result from solution of the Algebraic Riccati Equation  |
| $q$                                  | Coefficient in the Schweighart-Sedwick equations (out-of-plane motion)   |
| $Q, R$                               | Weight matrices in the LQR formulation   |
| $R_e$                                | Earth's mean radius (6378.1363)  |
| $r$                                  | Orbit radius of the spacecraft in the nonlinear dynamic equations. ( $\sqrt{x^2 + y^2 + z^2}$ )                      |
| $r_{ref}$                            | Reference local-vertical/local-horizontal orbit radius   |
| $S$                                  | Drag surface's area  |
| $t$                                  | Time   |
| $U_x, U_y, U_z$                      | ECI components of the control input in nonlinear dynamic equations   |
| $U_d$                                | Vector that contains all desired control inputs in the CLS formulation   |
| $U_{ind}$                            | Vector that contains all individual drag accelerations in the CLS formulation  |
| $u_x, u_y, u_z$                      | LVLH components of the control input in Schweighart-Sedwick equations  |
| $u_{min,t}$                          | Lower bound for the drag acceleration experienced by the target  |
| $u_{min,i}$                          | Lower bound for the drag acceleration experienced by the $i^{th}$ chaser   |
| $u_t$                                | Drag acceleration experienced by the target  |
| $u_{c,i}$                            | Drag acceleration experienced by the $i^{th}$ chaser   |
| $\Delta u_i$                         | Relative drag acceleration between the target and the $i^{th}$ chaser  |
| $\Delta u_{i,max}, \Delta u_{i,min}$ | Upper and lower bounds for $\Delta u_i$  |
| $\hat{V}$                            | Spacecraft velocity unit vector with respect to Earth's atmosphere   |
| $V_{\perp,j}$                        | Component of spacecraft's velocity relative to Earth's atmosphere that is perpendicular to the $j^{th}$ drag surface |
| $X_i$                                | State vector for the $i^{th}$ chaser-target pair   |
| $x, y, z$                            | Position coordinates of a spacecraft with respect to the ECI reference frame   |
| $\dot{x}, \dot{y}, \dot{z}$          | Velocity components of a spacecraft with respect to the ECI reference frame  |
| $\Delta x, \Delta y, \Delta z$       | Relative position components of a Chaser with respect to the target  |

|   |   |
|---|---|
| $\Delta\dot{x}, \Delta\dot{y}, \Delta\dot{z}$ | Relative velocity components of a Chaser with respect to the target               |
| $\Delta d_i$                                  | Desired along-orbit separation between the $i^{th}$ chaser and the target         |
| $\Delta\theta_i$                              | Desired difference in true anomaly between the $i^{th}$ chaser and the target     |
| $\phi$  | Phase of the forcing term in out-of-plane motion in Schweighart-Sedwick equations |
| $\rho$  | Atmospheric density   |
| $\omega$                                      | Target's circular-orbit angular velocity  |

## REFERENCES

- <sup>1</sup> C. L. Leonard, W.M. Hollister, E.V. Bergmann, "Orbital Formationkeeping with Differential Drag." *Journal of Guidance, Control, and Dynamics*, Vol. 12, No. 1, 1989, pp. 108-113.
- <sup>2</sup> C. L. Leonard, "Formationkeeping of spacecraft via differential drag", *Thesis (M.S.), Massachusetts Institute of Technology, Dept. of Aeronautics and Astronautics*, 1986.
- <sup>3</sup> M. Horsley, S. Nikolaev and A. Pertica. "Small Satellite Rendezvous Using Differential Lift and Drag." *Journal of Guidance, Control, and Dynamics*, Vol. 36, No.2, 2013, pp. 445-453.
- <sup>4</sup> S.A. Schweighart and R. J. Sedwick, "High-Fidelity Linearized  $J_2$  Model for Satellite Formation Flight." *Journal of Guidance, Control, and Dynamics*, Vol. 25, No. 6, 2002, pp. 1073-1080.
- <sup>5</sup> R. Bevilacqua and M. Romano, "Rendezvous Maneuvers of Multiple Spacecraft Using Differential Drag Under  $J_2$  Perturbation" *Journal of Guidance, Control, and Dynamics*, Vol. 31, No. 6, 2008, pp. 1595-1607.
- <sup>6</sup> D. Perez, R. Bevilacqua, "Differential Drag Spacecraft Rendezvous using an Adaptive Lyapunov Control Strategy" *Acta Astronautica*, Vol 83, February – March 2013, pp. 196-207.
- <sup>7</sup> D. Ivanov, M. Kushniruk and M. Ovchinnikov, "Study of Satellite Formation Flying Control Using Differential Lift and Drag" *Acta Astronautica*, Vol.152, November 2018, pp. 88-100.
- <sup>8</sup> M. W. Harris and B. Açıkmese, "Minimum Time Rendezvous of Multiple Spacecraft Using Differential Drag" *Journal of Guidance, Control, and Dynamics*, Vol. 37, No. 2, 2014, pp. 365-373.
- <sup>9</sup> S. Varma and K. D. Kumar, "Multiple Satellite Formation Flying Using Differential Aerodynamic Drag" *Journal of Spacecraft and Rockets*, Vol. 49, No. 2, March-April 2012, pp. 325-335.
- <sup>10</sup> D. Guglielmo, S. Omar, R. Bevilacqua, L. Fineberg, J. Treptow, B. Poffenberger and Y. Johnson, "Drag De-Orbit Device: A New Standard Re-Entry Actuator for CubeSats" *Journal of Spacecraft and Rockets*, 2018.
- <sup>11</sup> S. F. Rafano and R. Bevilacqua, "High fidelity model of the atmospheric re-entry of CubeSats equipped with the Drag De-Orbit Device", *Acta Astronautica*, May 2018.
- <sup>12</sup> S. Omar, D. Guglielmo, R. Bevilacqua, "Drag De-Orbit Device (D3) Mission for Validation of Controlled Spacecraft Re-entry Using Aerodynamic Drag", *4<sup>th</sup> IAA Dynamics and Control of Space Systems Conference*, Vol. 163, Rome, Italy, 2017.
- <sup>13</sup> S. Omar, D. Guglielmo, G. Di Mauro, T. Martin and R. Bevilacqua, "CubeSat Mission to Demonstrate Aerodynamically Controlled Re-Entry using the Drag De-Orbit Device (D3)", *SmallSat Conference 2018*, Logan, UT, 2018.
- <sup>14</sup> E. Lavretsky and K. A. Wise, "Robust and Adaptive Control with Aerospace Applications" *Advanced Textbooks in Control and Signal Processing*, Springer, 2013.
- <sup>15</sup> H. Curtis, "Orbital Mechanics for Engineering Students", *Elsevier Aerospace Engineering Series*, 2005.
- <sup>16</sup> K. Alfriend, S. Vadali, P. Gurfil, J. How and L. Breger, "Spacecraft Formation Flying", *Elsevier astrodynamics Series*, 2010.